Effect of n- and p-type Doping on Coherent Phonons in GaN

Kunie Ishioka[1], Keiko Kato[1] ‡, Naoki Ohashi[1], Hajime Haneda[1], Masahiro Kitajima[1] § and Hrvoje Petek[2]

[1] National Institute for Materials Science, Tsukuba, 305-0047 Japan

[2] Department of Physics and Astronomy, University of Pittsburgh, Pittsburgh, PA 15260, USA

E-mail: ishioka.kunie@nims.go.jp

Abstract.

Effect of doping on the carrier-phonon interaction in wurtzite GaN is investigated by pump-probe reflectivity measurements using 3.1 eV light in near resonance with the fundamental band gap of 3.39 eV. Coherent modulations of the reflectivity due to the E_2 and the A_1(LO) modes, as well as the $2A_1$(LO) overtone are observed. Doping of acceptor and more so of donor atoms enhances the dephasing of the polar A_1(LO) phonon via coupling with plasmons, with the effect of donors being stronger. Doping also enhances the relative amplitude of the coherent A_1(LO) phonon with respect to that of the high-frequency E_2 phonon, though it does not affect the relative intensity in Raman spectroscopic measurements. We attribute this enhanced coherent amplitude to the transient depletion field screening (TDFS) excitation mechanism, which in addition to impulsive stimulated Raman scattering (ISRS), contributes to generation of the coherent polar phonons even for sub-band gap excitation. Because the TDFS mechanism requires photoexcitation of carriers, we argue that the interband transition is made possible at the surface with photon energies below the bulk band gap through the Franz-Keldysh effect.

PACS numbers: 78.30.Fs, 63.20.kd, 78.47.jg

‡ Present address: NTT Basic Research Laboratories

§ Present address:National Defense Academy

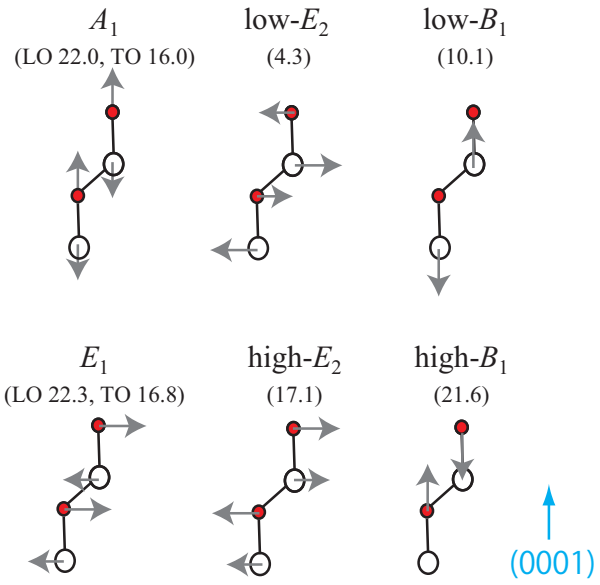

Figure 1. (Color Online.) Atomic displacements of the Γ-point phonons in wurtzite GaN [6]. Gallium and nitrogen atoms are colored white and red. Low-E_2 (low-B_1) and high-E_2 (high-B_1) denote the low- and high-frequency E_2 (B_1) modes, respectively. Numbers in parentheses denote the frequencies in THz obtained in previous studies [5, 6].

1. Introduction

Gallium nitride (GaN) is an important optoelectronic semiconductor with a direct-gap of 3.39 eV at room temperature. The optical properties of GaN depend on the rapid exchange of energy between the electronic and the lattice subsystems [1, 2, 3]. The wurtzite polymorph of GaN has optical phonon modes of A_1 (Raman (R) and infrared (IR) active), E_1 (R and IR active), E_2 (R active) and B_1 (silent) symmetries [4, 5, 6], whose atomic displacements are summarized in Fig. 1. The frequencies of the IR active A_1 and E_1 modes split into a longitudinal optical (LO) and a transverse optical (TO) components by the macroscopic electric field associated with the LO phonon. This electric field stiffens the force constant and thereby increases the LO frequency over the TO. For wurzite GaN the LO-TO splitting is greater than the $A_1 - E_1$ splitting, *i.e.*, $|\Omega_{LO}^{(A1)} - \Omega_{TO}^{(A1)}|$ and $|\Omega_{LO}^{(E1)} - \Omega_{TO}^{(E1)}| \gg |\Omega_{LO}^{(A1)} - \Omega_{LO}^{(E1)}|$ and $|\Omega_{TO}^{(A1)} - \Omega_{TO}^{(E1)}|$, indicating that the short-range forces are dominated by the electrostatic force rather than the interatomic anisotropy in [7].

Like in zinc-blende crystals, the LO phonons in wurtzite GaN can couple with plasmons to form LO phonon-plasmon coupled (LOPC) mode [4, 8, 9, 10, 11]. The A_1- and E_1-like LOPC modes can be distinguished by the detection geometry and optical polarization in Raman scattering measurements [10]. In general, the frequencies of the LOPC mode are given by the solution to the equation for the frequency-dependent

dielectric response of the lattice and the free electrons [4, 8, 11, 12]:

$$\varepsilon(\omega) = \varepsilon_\infty\Big[1 + \frac{\Omega_{LO}^2 - \Omega_{TO}^2}{\Omega_{TO}^2 - i\Gamma\omega - \omega^2} - \frac{\omega_p^2}{\omega^2 + i\gamma\omega}\Big] = 0, \tag{1}$$

where ε_∞ is the high frequency dielectric constant, γ and Γ, plasmon and phonon damping rates, and Ω_{LO} and Ω_{TO}, the LO and TO phonon frequencies. The plasma frequency,

$$\omega_p = \sqrt{\frac{ne^2}{m^*\varepsilon_0\varepsilon_\infty}}, \tag{2}$$

depends on the free carrier density, n their effective mass, m^*, and the vacuum dielectric constant, ε_0. For n-type GaN, the LOPC mode frequencies measured by Raman spectroscopy were found to follow the well-known undamped ($\gamma = \Gamma$=0) solutions of eq. (1) [8]:

$$2\omega_\pm^2 = \omega_p^2 + \Omega_{LO}^2 \pm [(\omega_p^2 + \Omega_{LO}^2)^2 - 4\omega_p^2\Omega_{TO}^2]^{1/2}. \tag{3}$$

For p-type GaN, by contrast, the coupling with plasmons was observed only as a slight broadening of the Raman LO peak without significant frequency shift [9]. The difference between the n- and p-type GaN was attributed to the heavy damping ($\gamma \gg \omega_p$) of the hole plasmon.

Detection of coherent optical phonons through transient transmission or reflectivity measurements enables monitoring the femtosecond time evolution of carrier-phonon coupling. Depending on the excitation photon energy, the excitation pulses may or may not add photocarriers to the valence and conduction bands. A previous transient transmission study from GaN(0001) surface with nonresonant 1.5 eV light [13] observed the two E_2-symmetry modes and the A_1(LO) mode. Only the polar A_1(LO) mode exhibited a pump power-dependent dephasing rate, confirming its strong Fröhlich interaction with the carriers photoexcited via a nonlinear three-photon process. No coherent LOPC mode, whether coupled with chemically doped or photoexcited carriers, was reported.

In the present study, we examine the electron-phonon coupling in differently doped GaN single crystals by transient reflectivity measurements with 3.1 eV light. With sub-band gap excitation we expect the coherent phonons to be excited mainly via nonresonant Raman process; the excitation of electron-hole pairs below the band gap resonance could be made possible only by Franz-Keldysh effect within the surface depletion region. We find that the dephasing rate of the A_1(LO) phonon is increased and its frequency upshifted by doping with donor atoms, whereas the dephasing rate is increased without any frequency shift by doping of acceptor atoms. We attribute our observation to the formation of the LOPC mode coupled with chemically doped carriers. We also observe the coherent amplitude of the A_1(LO) phonon to be enhanced significantly by the doping. Comparison with Raman spectra of the same samples suggests photoexcited ultrafast current in the surface depletion region is responsible for the enhancement.

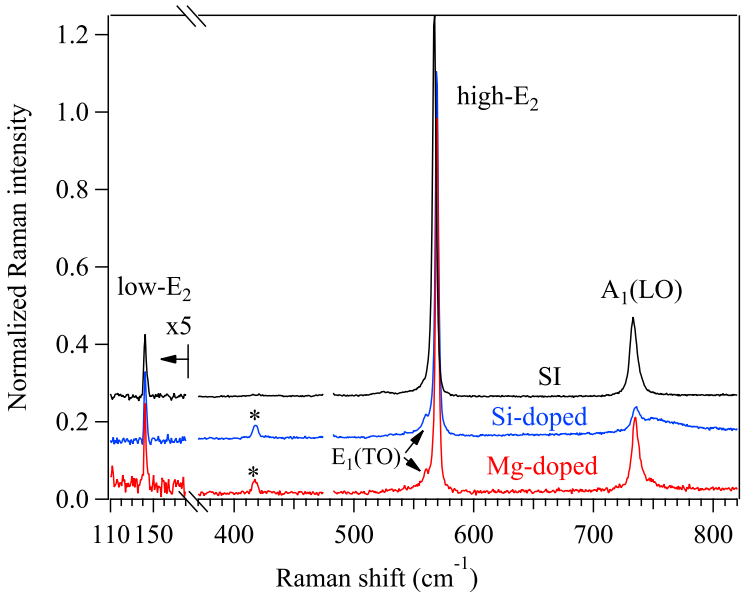

Figure 2. (Color Online.) Raman spectra of the differently doped GaN samples. The Raman intensities are normalized by the height of the high-E_2 phonon peak. Traces are offset for clarity. Asterisk (*) indicates the A_{1g} phonon of the sapphire substrate.

2. Experimental

The samples studied are GaN single crystal wurtzite polymorphs grown by metal organic chemical vapor deposition (MOCVD) on (0001)-oriented sapphire substrates [14]. The nominally undoped GaN layer is 50 μm thick and has a defect concentration of $\sim 1 \times 10^{16}$cm^{-3}, which makes it slightly n-type. The Si-doped n-type GaN film of 3.4 μm thickness is grown with Si concentration of $\sim 1 \times 10^{18}$ cm^{-3} on a 1.6 μm thick undoped buffer layer. The p-type GaN film of 0.5 μm thickness is grown with Mg doping concentration of $\sim 1 \times 10^{18}$cm^{-3} on a 5 μm thick undoped layer. Si and Mg are typical n- and p-type dopants in GaN [15, 16]. For comparison we also investigate an (0001)-oriented semi-insulating (SI) GaN single crystal of 1mm thickness (Kyma Technologies Inc.).

Pump-probe reflectivity measurements are performed with optical pulses with ~10 fs duration, 400 nm wavelength (3.1 eV energy), and 70 MHz repetition rate. Only a very small fraction ($\sim 0.1\%$) of the optical pulse spectrum exceeds the fundamental gap of GaN. Linearly polarized pump and probe beams are incident with angles of 20° and 5° from the surface normal. In this near back-reflection geometry from the (0001) surface, only the E_2 and A_1(LO) modes are dipole-allowed by the Raman scattering selection rules, which also dominate the generation and detection of coherent phonons [17]. The pump-induced change in the reflectivity ΔR is measured by detecting the probe beam reflected from the sample surface (isotropic detection) and accumulating the signal in a digital oscilloscope while scanning the time delay between the pump and the probe pulses at 20 Hz (fast scan).

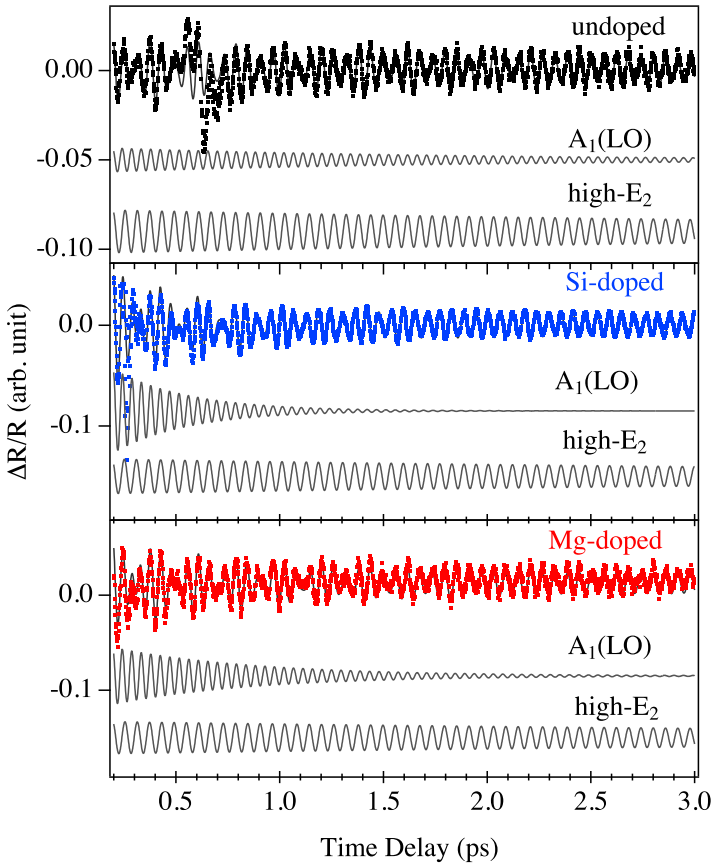

Figure 3. (Color Online.) Oscillatory parts of transient reflectivity responses $\Delta R/R$ (dots) and their decomposition into components due to the coherent A_1(LO) and high-E_2 modes (solid curves) for differently doped GaN samples.

Separate Raman scattering measurements on the same samples are performed in back-reflection geometry using a Raman microscope with nonresonant 532-nm (2.3-eV) excitation. The low-E_2, high-E_2 and A_1(LO) phonons are observed at 142, 569 and 736 cm^{-1}, as shown in Fig. 2; these comprise all the fundamental phonon modes allowed in the back-scattering geometry from the (0001) surface. For the Si- and Mg-doped samples the A_1(LO) peak splits into two, *i.e.*, the A_1(LO) phonon coupled with plasmons (A_1-like LOPC mode) from the doped layer and the bare A_1(LO) phonon from the undoped buffer layer [4, 8, 9, 10, 11]. For the thin film samples small Raman peaks from the dipole-forbidden E_1(TO) phonon of GaN and from the sapphire substrate are also observed at 561 and 417 cm^{-1}.

3. Results and discussion

Figure 3 compares the pump-induced reflectivity change $\Delta R/R$ of differently doped GaN samples. After photoexcitation at $t = 0$, the reflectivity oscillates with a clear beating pattern. The beating is mainly contributed by the high-frequency E_2 mode at 17 THz

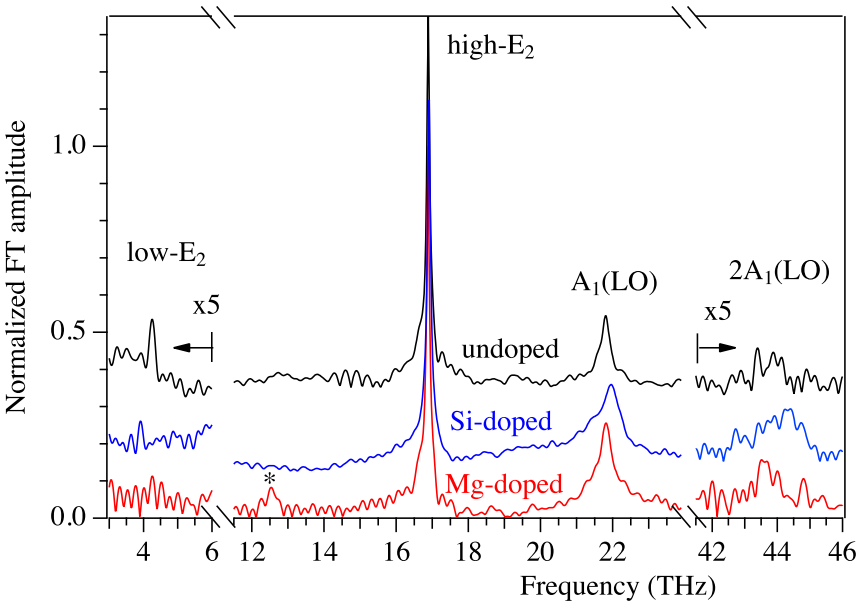

Figure 4. (Color Online.) Fourier transformed (FT) spectra of the oscillatory reflectivity change of differently doped GaN samples. The FT amplitude is normalized by the height of the high-E_2 phonon peak. Traces are offset for clarity. Asterisk (*) indicates the A_{1g} phonon of the sapphire substrate.

and the A_1(LO) mode at 22 THz, as shown in the Fourier transform (FT) spectra in Fig. 4. The individual oscillation components extracted by fitting the time-domain data to a sum of damped harmonic oscillations:

$$\frac{\Delta R(t)}{R} \simeq \frac{\Delta R_A}{R} \exp(-\Gamma_A t) \sin(2\pi\Omega_A t + \psi_A) + \frac{\Delta R_E}{R} \exp(-\Gamma_E t) \sin(2\pi\Omega_E t + \psi_E), \quad (4)$$

are also shown in Fig. 3. The observation of the E_2 and A_1-symmetry modes in the near back-reflection configuration is expected from the Raman selection rules [13, 5]. We also observe a weak low-E_2 mode at 4 THz and an overtone of the A_1(LO) phonon ($2A_1$(LO)) at 44 THz, as shown in Fig. 4. The small amplitude of the $2A_1$(LO) mode is in contrast to the resonant Raman spectrum at wavelengths shorter than 380 nm, which was found to be dominated by the overtones up to 7th [10, 18, 19]. Because our measurement system has sufficient bandwidth to detect the coherent response with bandwidth exceeding 100 THz [20], the weak overtone signal can be attributed to a pre-resonant response to photoexcitation at 400 nm. our observation thus indicates that the resonant effect is negligible with photoexcitation at 400 nm. The origin of the $2A_1$(LO) mode must be different from the recently reported harmonic frequency comb generation in Si through the amplitude and phase modulation of the reflected light within the optical skin depth, because the GaN samples are transparent to 3.1 eV light [20]. With increasing pump power, the amplitudes of all the coherent phonon modes increase linearly, while their dephasing rates and the frequencies exhibit no systematic pump-

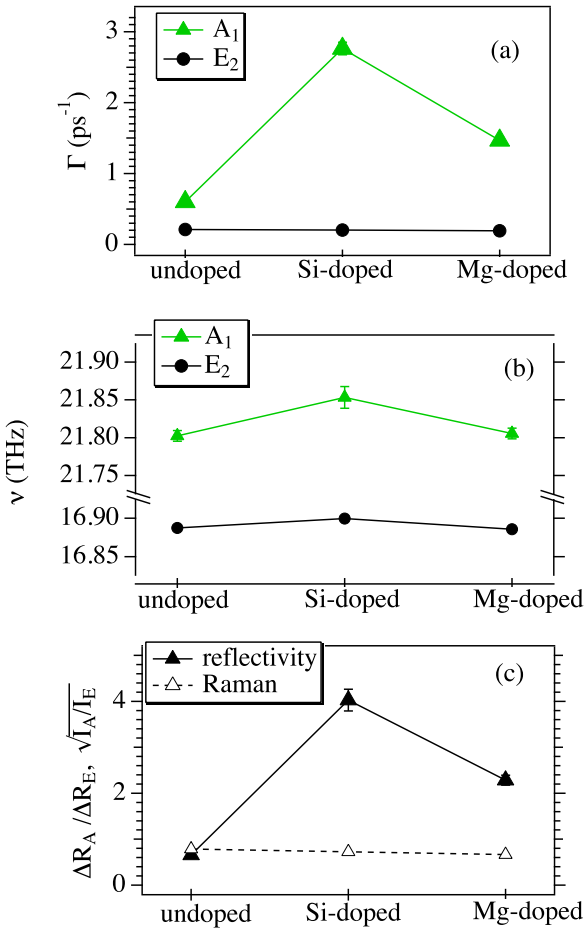

Figure 5. (Color Online.) (a) Dephasing rates and (b) frequencies of coherent high-E_2 and A_1(LO) phonons for differently doped GaN samples obtained from transient reflectivity measurements. (c) Relative coherent phonon amplitudes $\Delta R_A/\Delta R_E$ and square root of the Raman intensity ratios $\sqrt{I_A/I_E}$ for differently doped GaN samples. The Raman intensity I_A is the sum of the bare A_1(LO) and the LOPC modes.

power dependence for all the GaN samples examined in the present study. This confirms that multi-photon excitation of carriers is negligible under our photoexcitation with 3.1 eV light, in contrast to the near infrared photoexcitation in the previous transmission study [13].

Doping of GaN by Si and Mg impurities modifies the coherent A_1(LO) mode significantly through the coupling with plasmons, whereas the high-E_2 mode is hardly affected, as summarized in Fig. 5. This is because the polar A_1(LO) mode is much more susceptible to doping due to Fröhlich interaction than the non-polar E_2 mode [13, 18]. For the undoped sample, the dephasing rate of the A_1(LO) mode is $\Gamma_A \sim$0.6 ps^{-1} for the undoped sample, which is consistent with the lifetime obtained by time-resolved Raman spectroscopy at a low photocarrier density (10^{16} cm^{-3}) [3]. Doping of Si impurities (n-type) increases Γ_A to 2.8 ps^{-1} and upshifts the frequency Ω_A by 0.05 THz with respect to

that of the undoped sample. The Si-doping effect can be attributed to the formation of A_1(LO)-electron plasma coupled mode (A_1-like LOPC mode). The significant increase in Γ_A suggests that the plasmon damping cannot be neglected. Since ω_+ hardly varies with ω_p in the present low concentration regime, we calculate theoretical Raman scattering cross section due to deformation potential and electro-optic mechanisms [21] to estimate ω_p and γ. Theoretical spectrum reproduces the experimental FT spectrum reasonably when we assume ω_p ∼10 THz and γ ∼50 ps^{-1}. Doping of Mg (p-type) enhances Γ_A likewise, but the effect is smaller than n-doping, and Ω_A is hardly affected, as shown in Fig. 5(a,b). The experimental FT spectrum is reproduced by assuming ω_p ∼10 THz and γ ∼100 ps^{-1}. The obtained plasma frequencies are consistent with the carrier density $n \sim 1 \times 10^{18}$ cm^{-3} of the n- and p-type samples [eq. (2)], and the plasmon damping rates are comparable with those obtained in the previous Raman studies on similarly doped n- and p-type GaN [4, 11]. Our observations confirm that the coupling of the LO phonon with hole plasma is weaker than that with electron plasma due to the faster damping of holes [9, 11]. We note that the Faust-Henry coefficient used in the calculation was controversial among the previous studies [4, 12, 11], and the values obtained in the present study should therefore give only semiquantitative estimations.

In general, the LO phonons can couple with both chemically doped and photodoped electrons and holes. In the present study, however, we consider that the LO phonons couple mainly with chemically doped electrons and holes for Si- and Mg-doped samples, because we observe comparable line width for the A1-like LOPC peak in our Raman scattering spectra [Fig. 2]. We note that in the Raman spectra we clearly see the double peak due to the A_1-like LOPC mode and the bare A_1(LO) phonon from the doped and undoped buffer layers [Fig. 2], whereas in the time domain we observe only the A_1-like LOPC mode from the doped layer. This is probably because the coherent polar phonons are generated much more efficiently for doped layers than for undoped one, as we will discuss in the following paragraph.

Doping of Si or Mg also significantly enhances the amplitude of the A_1(LO) mode relative to that of the high-E_2 mode, i.e., $\Delta R_A/\Delta R_E$, whereas the Raman peak intensity ratio I_A/I_E is unchanged, as shown in Fig. 5(c). The difference can be explained in terms of the generation mechanism of the coherent A_1(LO) phonon. If all the coherent phonons are solely generated via impulsive stimulated Raman scattering (ISRS) [22], the relative amplitudes should be proportional to the square root of the relative Raman intensity $\sqrt{I_A/I_E}$ measured at the same wavelength. In resonant photoexcitation on polar semiconductors, however, coherent polar optical phonons can also be generated via transient depletion field screening (TDFS) mechanism [23], in which ultrafast screening by photoinjected current induces an abrupt change in the surface built-in field [Fig. 6(a)]. In the present study, photocarriers cannot be generated in the bulk GaN, since the photon energy is slightly below the fundamental band gap. Nevertheless, in the surface depletion region of n-doped GaN, the steep band bending can induce tails of the valence and conduction bands of about 0.1 eV through the Franz-Keldysh effect [24], as schematically illustrated in Fig. 6(b). This would allow a small but finite fraction of the

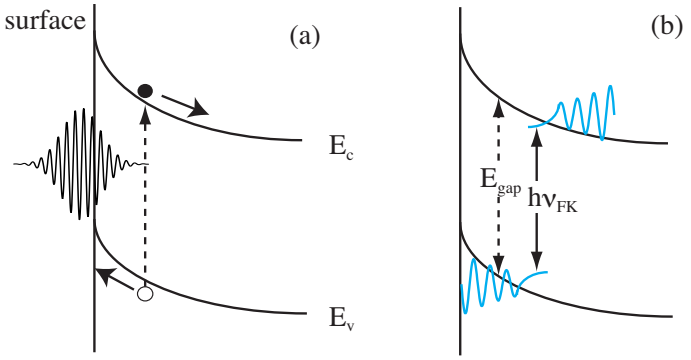

Figure 6. (Color Online.) Schematic illustrations of the band structure of an n-type semiconductor surface. (a) Photoinjected current screens the built-in surface field and excites coherent polar phonons via TDFS [23]. (b) Franz-Keldysh effect involving the coupling between the tails of the electron and hole wavefunctions causes the interband transition at an energy $h\nu_{FK}$ smaller than the band gap E_{gap} [24].

3.1 eV light to excite the interband transition. The photoexcited electrons would drift deeper into the bulk region, and thereby generate coherent A_1(LO) phonons by TDFS and form the LOPC mode. We thus attribute the enhancement in the coherent LOPC amplitude by n-doping to the additional TDFS generation. Similar mechanism can be at work at the surface of a p-type semiconductor. The difference in the generation efficiency for the n- and p-doped samples depends on the position of the Fermi level pinning with respect to the band gap edges.

4. CONCLUSION

We have investigated the effect of n- and p-type doping on carrier-phonon dynamics of GaN under photoexcitation with 3.1 eV light. The dephasing rate, the frequency and the amplitude of the polar A_1(LO) phonon are modified by coupling with chemically doped electron (hole) plasma for n-doped (p-doped) sample, with the effect of n-doping greater than that of p-doping. Because the photon energy is slightly short of the band gap of bulk GaN, photoexcitation is made possible by Franz-Keldysh effect only at the surfaces with steep band bending. Such photoexcitation enables the generation of coherent A_1(LO) phonons via transient screening in the surface depletion field. Our study reveals the complex interactions between the carriers and lattice affecting the optical properties of GaN in the surface band bending region.

Acknowledgments

This research was partially supported by NSF CHE-1213189 grant.

[1] A. Kasic, M. Schubert, S. Einfeldt, D. Hommel, and T.E. Tiwald. *Phys. Rev. B*, 62(11):7365–7377, 2000.

[2] D.Y. Song, M. Basavaraj, S.A. Nikishin, M. Holtz, V. Soukhoveev, A. Usikov, and V. Dmitriev. *J. Appl. Phys.*, 100(11):113504, 2006.
[3] K. T. Tsen, J. G. Kiang, D. K. Ferry, and H. Morkoc. *Appl. Phys. Lett.*, 89:112111, 2006.
[4] T. Kozawa, T. Kachi, H. Kano, Y. Taga, M. Hashimoto, N. Koide, and K. Manabe. *J. Appl. Phys.*, 75(2):1098, 1994.
[5] T. Azuhata, T. Sota, K. Suzuki, and S. Nakamura. *J. Phys.: Condens. Matter*, 7(10):L129, 1995.
[6] J.M. Zhang, T. Ruf, M. Cardona, O. Ambacher, M. Stutzmann, J.M. Wagner, and F. Bechstedt. *Phys. Rev. B*, 56(22):14399, 1997.
[7] C.A. Arguello, D.L. Rousseau, and S.P.S. Porto. *Phys. Rev.*, 181(3):1351–1363, 1969.
[8] P. Perlin, J. Camassel, W. Knap, T. Taliercio, J. C. Chervin, T. Suski, I. Grzegory, and S. Porowski. *Appl. Phys. Lett.*, 67:2524, 1995.
[9] H. Harima, T. Inoue, S. Nakashima, K. Furukawa, and M. Taneya. *Appl. Phys. Lett.*, 73:2000, 1998.
[10] N. Wieser, M. Klose, R. Dassow, F. Scholz, and J. Off. *J. Crystal Growth*, 189-190:661, 1998.
[11] F. Demangeot, J. Frandon, M. A. Renucci. N. Grandjean, B. Beaumont, J. Massiers, and P. Gibart. *Solid State Commun.*, 106:491, 1998.
[12] C. Wetzel, W. Walukiewicz, and J.W.A. III. In F. Ponce, T.D. Moustakas, I. Akasaki, and B. Monemar, editors, *Proc. Mat. Res. Soc. Symp.*, volume 449, page 567. MRS, 1996.
[13] K. J. Yee, K. G. Lee, E. Oh, and D. S. Kim. *Phys. Rev. Lett.*, 88:105501, 2002.
[14] Y.-Z. Yao, T. Ohgaki, N. Fukata, Y. Adachi, Y. Wada, H. Haneda, and N. Ohashi. *Scripta Materialia*, 62(7):516–519, 2010.
[15] S. Nakamura, T. Mukai, and M. Senoh. *Jpn. J. Appl. Phys.*, 31:2883, 1992.
[16] H. Amano, M. Kito, K. Hiramatsu, and I. Akasaki. *Jpn. J. Appl. Phys.*, 28:L2112, 1989.
[17] K. Ishioka, A.K. Basak, and H. Petek. *Phys. Rev. B*, 84(23):235202, 2011.
[18] A. Kaschner, A. Hoffmann, and C. Thomsen. *Phys. Rev. B*, 64(16):165314, 2001.
[19] W. H. Sun, S. J. Chua, L. S. Wang, and X. H. Zhang. *J. Appl. Phys.*, 91(8):4917, 2002.
[20] M. Hase, M. Katsuragawa, A.M. Constantinescu, and H. Petek. *Nature Photonics*, 6(4):243–247, 2012.
[21] M. V. Klein. Electronic raman scattering. In M.Cardona, editor, *Light Scattering in Solids I*, page 147. Springer, Berlin, 1983.
[22] L. Dhar, J. Rogers, and K. A. Nelson. *Chem. Rev.*, 94:157, 1994.
[23] M. Först and T. Dekorsy. Coherent phonons in bulk and low-dimensional semiconductors. In S. De Silvestri, G. Cerullo, and G. Lanzani, editors, *Coherent Vibrational Dynamics*, page 129. CRC, Boca Raton, 2007.
[24] A. Cavallini, L. Polenta, M. Rossi, T. Stoica, R. Calarco, R. J. Meijers, T. Richter, and H. Luth. *Nano Lett.*, 7(7):2166, 2007.